Beam Engineering for Advanced Measurements Co.
Orlando, Florida

Thin-Film Broadband Large Area Imaging System

NIAC Phase I Final Report

Nelson Tabirian, Principal Investigator

Summary

Our Phase I program has addressed the possibility of applying thin-film diffractive waveplate technology to large aperture space-based telescopes for such applications as exoplanet imaging and spectral analysis. The major benefit that may be achievable with this technology is to make very large aperture, diffraction limited, space-based imaging possible at a small fraction of the cost that would be incurred with alternative methods using conventional optics including a reflective primary mirror. We have developed a point optical design that is predicted to achieve diffraction-limited imaging in the visible wavelength band over a bandwidth of ±8% of the center wavelength.

The geometrical phase modulation introduced by waveplate lenses is wavelength independent – resulting in the broadband nature of these new generation components and feasibility for having near 100% diffractive efficiency over very broad range of wavelengths. Since, however, the diffraction angle depends on wavelength, the bandwidth of a diffraction-limited astronomical telescope with a flat, transmissive primary element may be limited by chromatic aberration. Finding solutions to the problem of chromatic aberrations was an important task during Phase I of our program. Luckily, unlike conventional mirrors and lenses, our novel optical components provide a myriad of opportunities to deal with the problem.

While alternative diffractive optical techniques for large-aperture space-based imaging, there has been only a small effort devoted to DW lenses and mirrors for this application. In view of the critical potential advantages of this technology over the alternatives, we believe that these techniques merit further investigation for such applications.

1. Background and previous state-of-the-art

Our proposed concept for a large-aperture space-based imaging telescope is founded on the emerging technology of diffractive waveplate (DW) optical components, including DW lenses and mirrors. The material of choice for these components for many applications is liquid crystal polymer (LCP). The state of the art in LCP DW lenses at BEAM Engineering for Advanced Measurements (BEAM Co.) is illustrated in Figure 1. With this technology, lenses can be fabricated as films with a thickness of the order of the wavelength of the diffracted electromagnetic radiation.
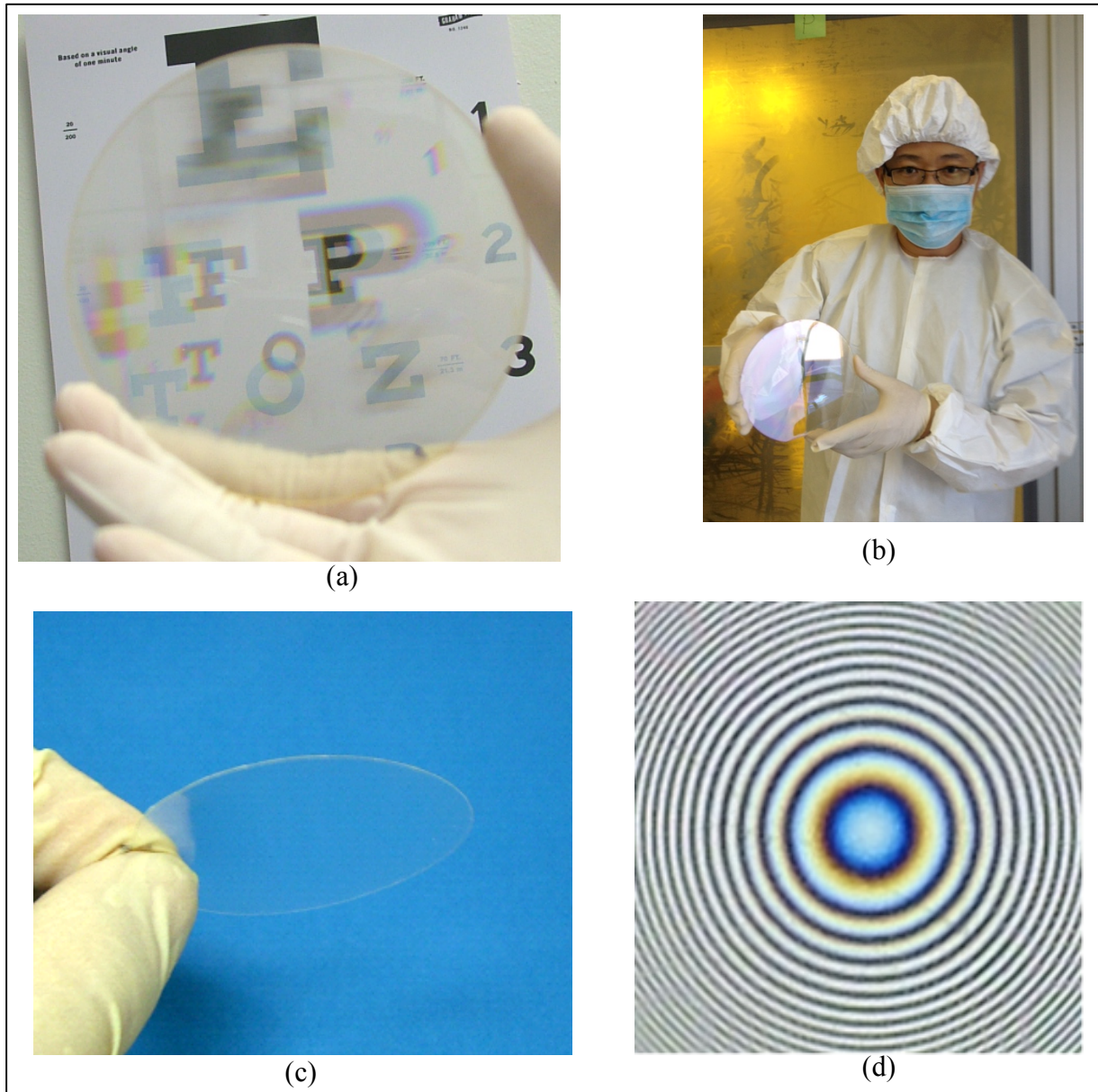

Figure 1. State of the art in DW lenses. (a) Illustration of diffraction by a DW lens; (b) 150 mm diameter DW lens; (c) DW lens as a coating on a polymer film; (d) photo of DW lens between linear polarizers.

1.1 State of the art of diffractive waveplate technology

The fundamental principles on which DW technology is based were introduced by S. Pancharatnam in the 1950s in the context of optics [1,2], and elaborated upon in a more general context by M. Berry in the 1980s and 1990s [3]. The fabrication of practical optical devices implementing the fundamental principles introduced by these early workers was delayed primarily by a lack of suitable materials and fabrication processes.

Much of the earliest work on DW optics concentrated on devices in which the DW grating structure was linear in the plane of the DW structure. More recently, BEAM Co. has collaborated with JPL in development of a particular type of DW optical element called the vector vortex waveplate (VVW) for application to coronagraphy[4,5,6]; others have also participated in this application of DW technology [7]. An example of optical characterization of a VVW fabricated by BEAM Co. is shown in Figure 2.
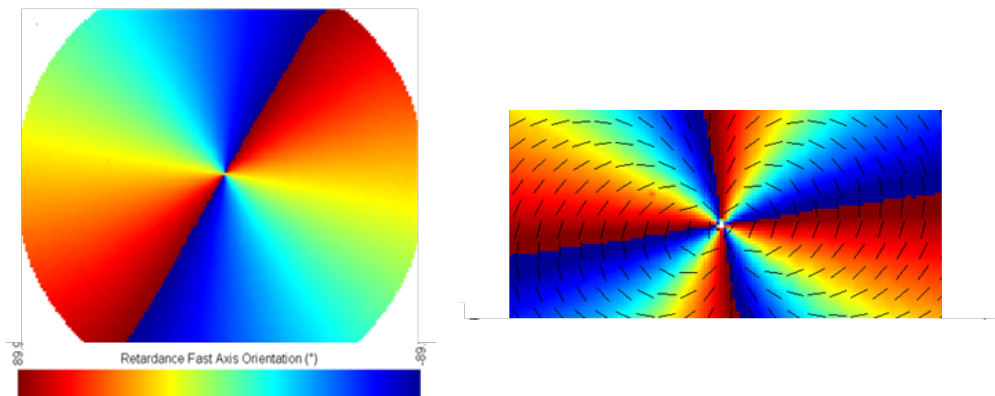

Figure 2. Orientation of optical axis distribution in sample VVWs as measured with Mueller Matrix Polarimeter.

Only quite recently have the more complex optical axis patterns required for optical lenses become feasible, and been reported by BEAM Co. in publications [8,9,10,11] and presentations [12,13,14,15,16,17,18]. This is an active area of research elsewhere as well [19,20,21].

1.2 Alternative diffractive technologies for space-based imaging

Diffractive alternatives to conventional optics for large-aperture space-based imaging have been previously proposed and developed to some extent. Here we will reference two such alternative to compare and contrast with DW technology. These two alternative are the use of diffractive Fresnel lenses and Fresnel zone plates.

The use of a diffractive Fresnel lens as the primary collection element in space-based telescopes was proposed in 1998-1999 [22,23]. In some of the early work on large-aperture diffractive Fresnel lenses, it was assumed that the lenses would have a continuous structure, thus providing the highest possible diffraction efficiency at the design wavelength, as well as the

possibility of multiband operation. However, later developments involved binary Fresnel lenses, primarily because of the extreme difficulty of fabricating diffractive Fresnel lenses with a continuous profile in optics of the size of interest for space-based imaging. As a result, even after the expenditure of $37M [24], the thin-film polymer optics tested [25] under the DARPA MOIRE program were binary Fresnel lenses, not continuous Fresnel lenses. In parallel with the demonstration of imaging with a binary Fresnel primary, processes were developed that make it possible to fabricate relatively large size, four-level diffractive Fresnel lenses [26], significantly increasing the diffraction efficiency.

Another approach that has been proposed for a diffractive primary in large-aperture space-based imaging is the use of a Fresnel zone plate. A subscale ground-based prototype of a proposed space-based telescope employing a Fresnel zone plate primary optic has recently been fabricated and tested [27]. A variant of this concept, sometimes referred to in the literature as a "photon sieve," in which the clear areas of the zone plate are circular, has been constructed for a demonstration of space-based, very narrowband imaging of spectral lines emitted by the sun [28].

All of the above-noted diffractive techniques that have been suggested for large aperture space-based imaging have the potential advantage of requiring only a thin primary optical element, and therefore also the potential to drastically reduce the weight of very large aperture space-based imagers. Each of these techniques has advantages and disadvantages relative to the others. Since the Fresnel lens and Fresnel zone plate have been known for many years, some of their strengths and weaknesses are better known than those of the DW approach, which has received minimal study for this application. In our study of the possibility of the using DW elements for this application, the following advantages seem apparent of DW technology over other diffractive techniques, and justify continued study of this technique for space-based imaging:

1. <u>Practicality of fabrication of large aperture components at affordable cost</u> - The fabrication of both binary and multilevel transmissive Fresnel lenses requires much more extensive facilities and equipment than does the fabrication of DW lenses of the same size. An indication of this is that it has been plausibly claimed that Lawrence Livermore National Laboratory has "…the only facility in the world that can make precision diffractive optics of more than a few centimeters in diameter."[29] This statement may be true for diffractive Fresnel lenses, but it is certainly not true for DW technology. This advantage of DW waveplate technology seems to be inherent, in the sense that with this technology, arbitrary DW patterns can be written optically, whereas Fresnel lenses must be fabricated by means of photolithographic or precision mechanical methods.

2. <u>Optical efficiency</u> - The upper limit on the diffraction efficiency for each circular polarization of light is 100% for a DW lens, and the focal length for each circular polarization is (-1) times the focal length for the other circular polarization. Therefore, for unpolarized light such as that from a distant exoplanet, the upper limit on overall efficiency is 50% for the focused component. However, as we recently reported [9], the upper limit for an appropriately-designed pair of DW lenses is 100%.

The only other diffractive technique of which we are aware that has a theoretical upper limit of 100% on optical efficiency (after Fresnel reflective losses are compensated) is the continuous Fresnel lens. As of now, this type of lens is not feasible at the aperture sizes needed for such missions as exoplanet imaging. The theoretical upper limit on the optical efficiency of any binary Fresnel lens, the type of lens used for imaging demonstrations [25] on the MOIRE program after the expenditure of $37M, is 40%, and the upper limit for the Fresnel zone plate is only 10%.

The possibility of high-efficiency polarization insensitive imaging with DW lenses is discussed in the Results section below.

3. <u>Broadband and multiband capability</u> - Unique among the diffractive techniques discussed above, DW lenses have an extra degree of freedom in that the axial structure of the optical axis can be structured in such a way as to modify the spectral characteristics of the diffraction efficiency. To date, this degree of freedom has primarily been used to achieve broader spectral coverage than can be achieved with a DW coating in which the optical axis orientation of the anisotropic material of which the DW is comprised has no axial dependence. The achievement of broadband diffraction with DW coatings having an axial dependence in the optical axis orientation is discussed in Ref. [11], and the axial structure is illustrated in Figure 3. It seems likely that this degree of freedom can be used to achieve multiband capability as well. This possibility will be discussed in the Results section below.
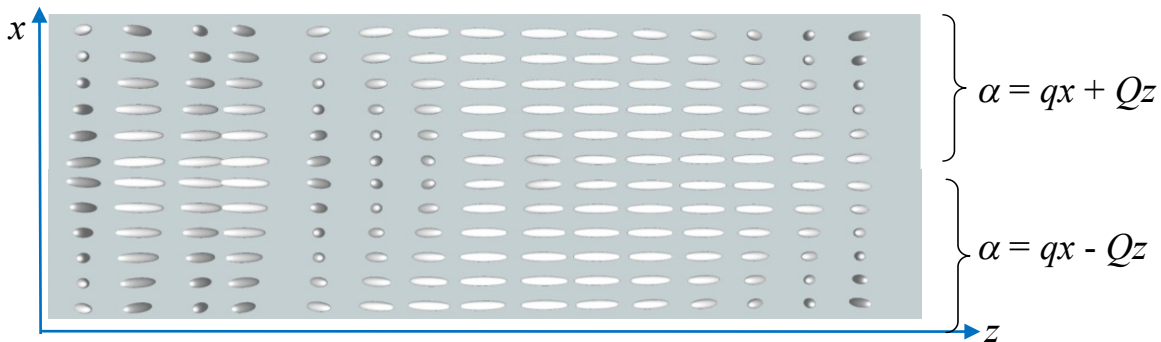

Figure 3. Axial dependence of optical axis orientation in a cycloidal DW designed for broadband operation. The coordinate *x* is in one of the two directions perpendicular to the thin-film layer; the coordinate *z* is in the direction perpendicular to the plane of the device. For illustration, a cycloidal grating is shown, for which the azimuthal orientation angle *α* of the optical axis of the anisotropic material comprising the DW device varies in only one of the two lateral dimensions, but the same axial dependence can also be used to achieve broadband operation in other DW devices including lenses.

4. <u>Continuous structure</u> - Both Fresnel lenses and Fresnel zone plates have a discontinuous mechanical structure, whereas a DW lens has a continuous structure, with only modulation of the optical axis orientation. While we cannot at present quantify the potential advantage of this distinction in the fundamental structure of these three types of diffractive element, it seems likely that it will be extremely difficult or impossible to avoid small-angle scattering in these

discontinuous structures. Thus, for applications such as exoplanet imaging that are sensitive to small-angle forward scattering, some coronagraphic techniques for suppression of the image of the star around which the exoplanet is orbiting might be feasible with a DW lens, but not feasible with the alternative types of diffractive structure.

5. <u>Curved DW lenses and mirrors</u> - Unlike the situation with the other two types of diffractive structure mentioned above, it is relatively straightforward with DW technology to create diffractive patterns on curved components such as curved lenses and mirrors. This requires only that the optical axis pattern be optically written onto the curved surface, instead of onto a planar surface. As will be discussed in the Results section below, we put this possibility to use, at least conceptually, in our development of a design concept for a large-aperture DW telescope. We also demonstrated this capability, as also discussed in the Results section. Having the capability to create curved components allows a reduction in the number of optical elements, thereby resulting ultimately in a lower cost system.

.

1.3 Bandwidth extension using a corrector mirror with a DW coating

Previous work at BEAM Co. [11] has demonstrated that high efficiency, thin-film DW lenses can be used to focus electromagnetic radiation over a broad range of wavelengths . However, chromatic aberrations inherent in the diffractive nature of this type of lens limit the spectral bandwidth over which high spatial resolution can be achieved. Earlier, with respect to the feasibility of large-aperture telescopes for deep-space optical communication based on thin-film DW objective lenses, we had shown that the use of a single curved, diffractive secondary corrector mirror can partially overcome chromatic aberrations of the diffractive primary. The use of a single corrector increased the bandwidth over which the telescope achieved diffraction-limited spatial resolution by approximately three orders of magnitude over the diffraction-limited bandwidth of an uncorrected diffractive waveplate primary lens. An example of a conceptual design of such a telescope with a single corrector is shown in Figure 4.

Although an increase in bandwidth by three orders of magnitude is certainly helpful, this still left the diffraction-limited bandwidth at less than one nanometer for a center wavelength in the visible wavelength band. Such a narrow diffraction-limited bandwidth would severely limit light collection and therefore imager signal-to-noise ratio in any broadband imaging application. Therefore, the first priority of our Phase I study was to prove the feasibility of further increasing the spectral bandwidth by developing improved conceptual telescope designs.
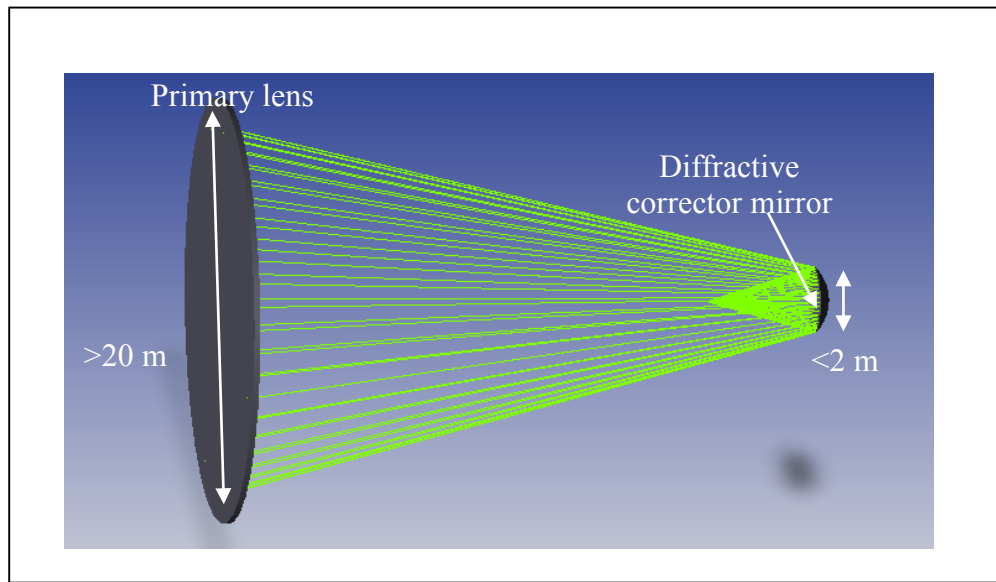
Figure 4. Diffractive corrector mirror increasing diffraction limited spectral bandwidth by a factor >1000 without loss of efficiency.

2. NIAC Phase I results

One of the major results of the Phase I study was the development of a design concept using DW components in the visible spectral band and a 20 meter diameter DW lens as the primary collection aperture, and performing at the diffraction limit in angular resolution over a bandwidth of ±8% of the central wavelength. This result is described in section 2.1. We also performed a preliminary tolerance analysis of this design, as described in section 2.2. Our design concept described in sections 2.1 and 2.2 required DW coatings on curved mirrors, and we have demonstrated the feasibility of such components by applying such coatings to a curved refractive lens as described in section 2.3.

As has been found for other diffractive techniques, size of the aft optics (that is, the optics behind the primary optical collector) are driven by the optical bandwidth over which the telescope is required to perform. We explore an option in section 2.4 of reducing the bandwidth below the ±8% achieved by the system analyzed in sections 2.1 and 2.2, thereby allowing a factor of four reduction in the diameter of the largest optical component in the aft optics.

The possibility of operating in multiple wavelength bands with a single system based on DW waveplate components is discussed in section 2.5. Finally, the use of polarization-insensitive imaging with very high optical efficiency using a pair of DW lenses as the primary optical assembly is discussed in section 2.6.

All the optical modeling described here was performed with the Zemax software package.

2.1 Spectral bandwidth improvement with dual-corrector design

We illustrate the results of our optical design studies with a wideband point design that includes two curved, reflective diffractive correctors, and with a circular primary diffractive lens of diameter D = 20 m. This results in an Airy radius of $1.22\lambda/D$ = 0.03 μrad at the center of the operating wavelength band. The point design achieves this angular resolution over the entire operating wavelength band, i.e. over a bandwidth of ±8% of the center wavelength. Figure 5 shows the optical layout.

Figure 4 illustrates the results of optical design modeling, showing that our telescope design concept with two corrector mirrors is capable of diffraction-limited angular resolution from 520 nm to 610 nm wavelength. Letting the nominal center wavelength be 565 nm, the diffraction-limited bandwidth is +/-8% of the nominal center wavelength.
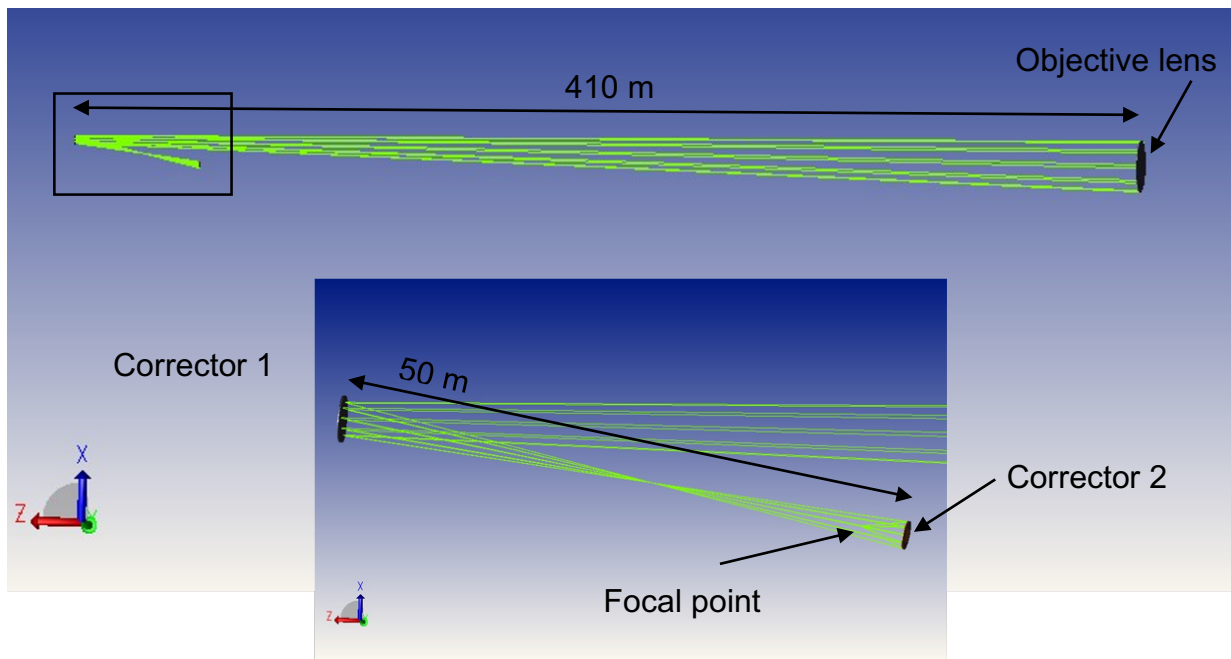
Figure 5. Telescope design concept with a diffractive waveplate primary lens 20 meters in diameter, and with two curved corrector mirrors with diffractive waveplate coatings.

Major dimensions of the primary lens and the two corrector mirrors in this two-corrector telescope design are shown in Table 1. The primary (objective) diffractive waveplate lens is flat, so the "Maximum sag" shown for this element in the table is zero. The first corrector mirror is nearly flat, with a maximum sag of only 22 mm over its 4 m diameter. The second corrector is "faster," with a sag of 150 mm over its 2.8 m diameter. While these aspherical optical components are by no means trivial, they are well within the state-of-the-art of fabrication techniques. Therefore they do not affect the fundamental feasibility of the design. The optical axis orientation pattern of the first corrector mirror is illustrated in Figure 6.The shapes of the two corrector mirrors are shown in Figure 7 and Figure 8.

Figure 9 and Figure 10 demonstrate the diffraction-limited character of the optical design illustrated in Figure 5. The design optimization was performed by minimizing the size of the point source image at each of 51 uniformly-spaced wavelengths from 500 nm to 600 nm. The ray trace results shown on the left side of Figure 9 are for the two limits of this wavelength range (i.e. for wavelengths of 500 nm and 600 nm) and for four additional intermediate wavelengths. For the on-axis case the RMS radius of the rays at the focal plane is 0.5 µm, compared with the Airy radius of 1.1 µm. Since the system focal length is 34 m, this Airy radius corresponds in the object space to an RMS radius of 0.015 µrad and an Airy radius of 0.032 µrad. This angular resolution is far superior to that of any existing telescope.

Table 1. Major dimensions of three optical components of space telescope

Optical component	Diameter (m)	Maximum sag (mm)
Primary diffractive waveplate lens	20	0
First corrector mirror	4	22
Second corrector mirror	2.8	150

(a)   (b)
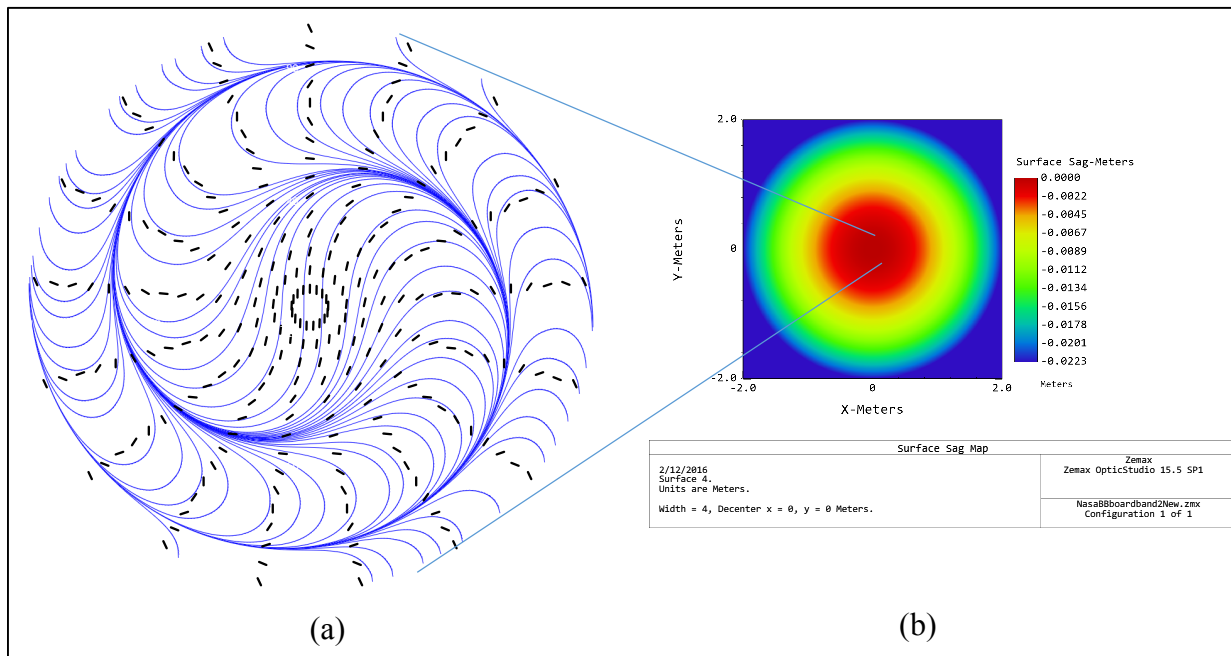
Figure 6. Optical axis pattern and sag of first corrector mirror. (a) Pattern near the center of the lens; (b) surface sag over the entire area of the mirror. The diameter of the mirror is 4 meters.
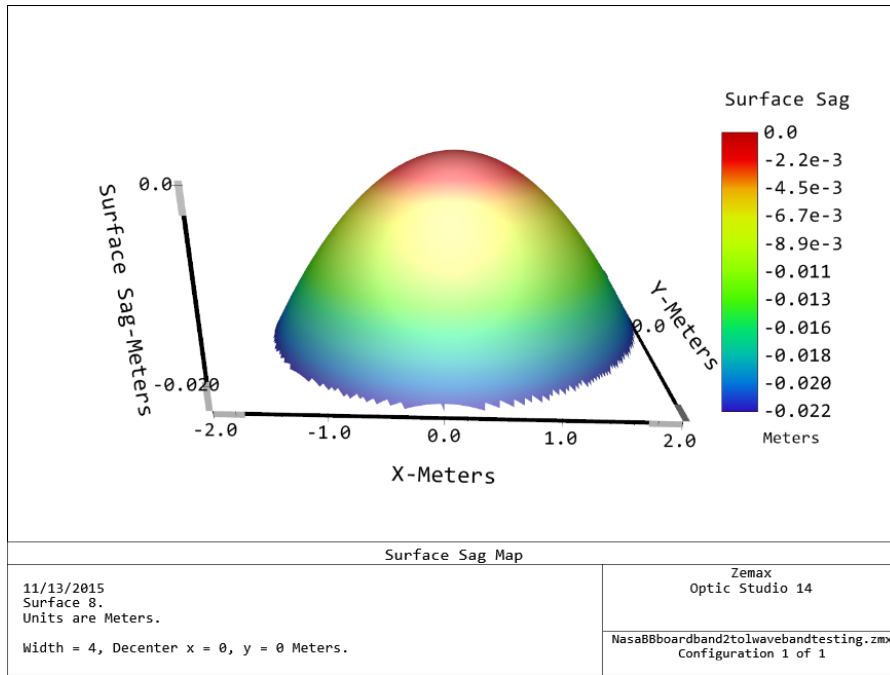
Figure 7. Shape of first corrector mirror in space telescope design concept. Diameter of the corrector is 4 m, and axial sag at the center relative to the edge is 22 mm.
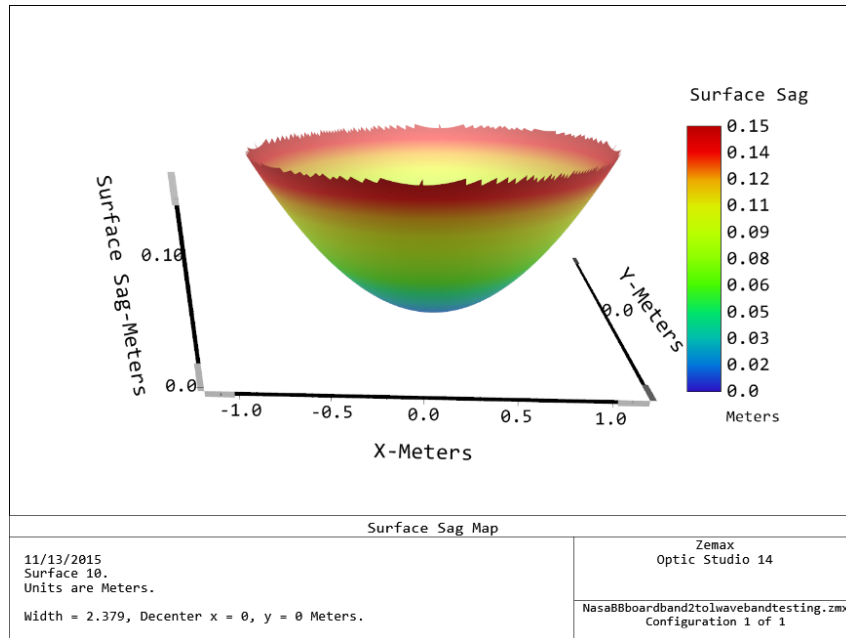

Figure 8. Shape of second corrector mirror in space telescope design concept. Diameter of corrector is 2.4 m, and axial sag at the center relative to the edge is 150 mm.

On axis   1.7 microradians off axis
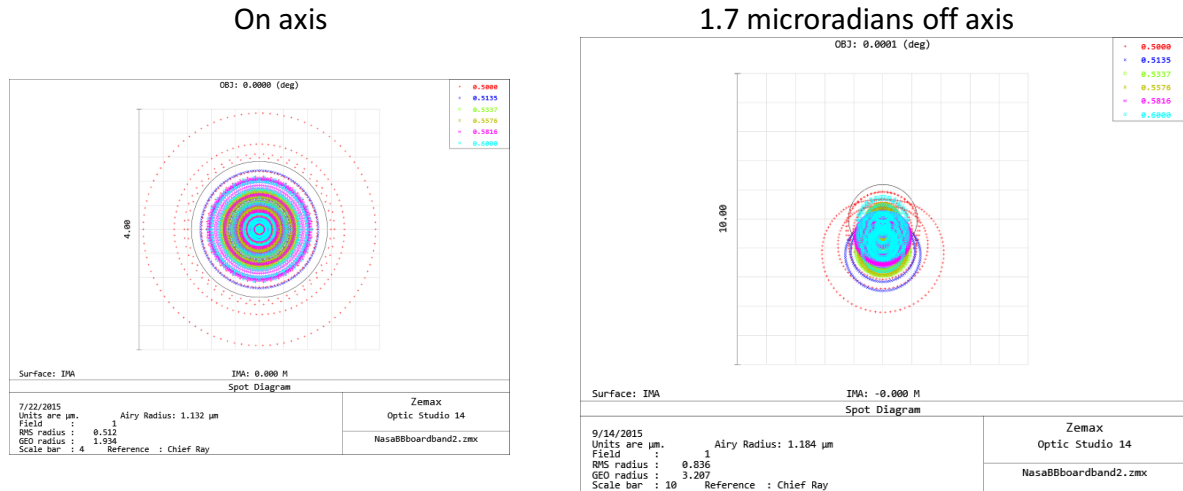
Figure 9. Ray tracing results for the baseline space telescope design, for the case in which the target is on axis, and the case in which the target is 1.7 µrad off axis.
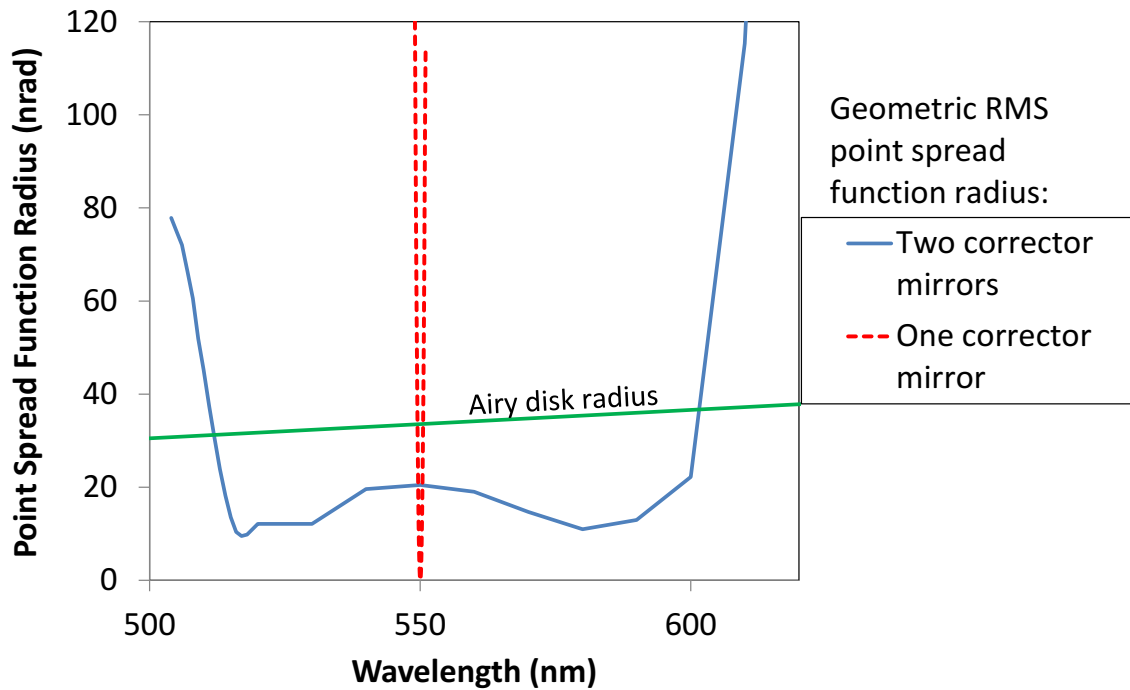

Figure 10. Dependence of telescope point spread function radius on wavelength. The PSF radius has been converted to object-space angle by dividing by the system effective focal length, equal to EFL = 34 m.

We also performed ray tracing for the point design at off-axis field points. For example, the ray trace results on the right side of Figure 9 are for an object space field angle of 1.7 µrad. At this field angle, the angular resolution is still diffraction-limited. While 1.7 µrad is a small field angle for conventional telescopes, it is at a field angle more than 100 times the on-axis RMS spot radius of the point design. We have only optimized the design for angular resolution at the center of the field, so it is almost certainly possible to significantly increase the angular field over which imaging is diffraction-limited without major modifications such as increasing the number of optical components.

While some imaging and spectral analysis missions are expected to require a diffraction-limited spectral bandwidth of the order of +/-10 percent of the center wavelength, some other applications such as optical communications require only a much narrower wavelength region over which the telescope must achieve diffraction-limited spatial resolution. Thus, the simpler single-corrector design shown in Figure 4 should be adequate for such narrowband applications.

The angular resolution shown in Figure 9 and Figure 10 is at least 10 times better than for any existing space telescope. Thus, the telescope of our design concept would achieve a given linear resolution at exoplanet systems at ranges at least 10 times longer than any existing telescope. Therefore, any mission whose success depends on achieving a given linear dimensional resolution at the target star system could achieve mission success over a volume of space 1000 times larger with the telescope characterized by these figures that could be achieved by any existing space telescope. Assuming a uniform density of planets supporting life in our region of the galaxy, and assuming that successful detection of life depends on achieving a certain linear dimensional resolution at the exoplanet, the expected number of planets for which life could be detected would be 1000 times greater with a telescope whose angular resolution is described by Figure 9 and Figure 10 than the number expected for any existing space telescope.

It would be desirable if the linear extent of the telescope were smaller than the several hundred meter linear extent of the telescope layout shown in Figure 5. However, so far our optical modeling has indicated that the corrector mirrors become problematic from the point of view of manufacturability when the overall length of the telescope is reduced much below that of Figure 5. This is illustrated in Figure 11, which shows ray traces near the second corrector for a design with an f/25 primary such as the design of Figure 5, and for a design with an f/10 primary.

As is demonstrated by Figure 11, the curvature of the second corrector mirror becomes very pronounced when the f-number of the primary diffractive waveplate lens is significantly less than 25.
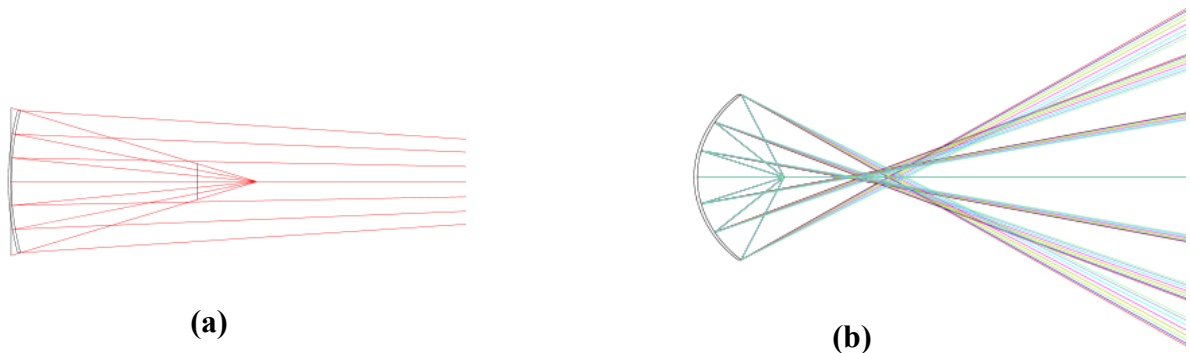
Figure 11. Ray trace for two telescope layouts, both with 20 meter diameter primary diffractive waveplate lens, (a) with f/25 primary, (b) with f/10 primary.

2.2 Preliminary optical tolerance analysis of dual-corrector design

Figure 12 through Figure 14 show results from a preliminary optical tolerance analysis of the telescope design concept described above (with f/25 primary). Each of these figures shows a spot diagram in the focal plane of the telescope, consisting of a diagram of the positions in the focal plane at which rays of light incident on the primary collection optic from long range intersect the focal plane. The dimensions shown on these figures are micrometers. Since the effective focal length (EFL) of the telescope is 34 m, one micrometer in the focal plane corresponds to 29 nrad in the object space.

Each of these figures includes an output from Zemax indicating that the Airy radius (radius of the first Airy dark ring) for the design is 1.13 µm. This parameter, characterizing the diffraction limit on angular resolution, is consistent with a reference wavelength of 0.535 µm, a primary aperture diameter of 20 m, and system EFL = 34 m.

For purposes of our preliminary tolerance analysis, we use the term "aft optics assembly" to refer to the structure containing the two corrector mirrors and the focal plane assembly. We will assume for this preliminary analysis that the aft optics assembly can be treated as a rigid body, and will not account for optical tolerances within this assembly.

The left side of Figure 5 shows the ray trace results for the case without any tilts or decentering in the design, and for six wavelengths from 0.5 µm to 0.6 µm. Except for the rays at 0.5 µm, all of the rays generally are incident on the focal plane within about 1 µm of the axis, consistent with Figure 4 which shows a geometric blur spot radius referred to the object space of less than 30 nrad RMS for all wavelengths except those near 0.5 µm.

Figure 12 shows the impact on the focal plane blur spot of displacing the 20 meter diameter primary diffractive lens laterally with respect to the aft optics assembly by 0.1 mm. Although the blur spots for each of the individual wavelengths are not significantly affected by this displacement, the polychromatic blur spot is smeared significantly (RMS radius almost doubled)

due to displacement of each monochromatic blur spot relative to the others. This result suggests that at least with our current telescope design concept, a tight tolerance must be achieved in the transverse alignment of the primary optic and the aft optics assembly if the diffraction-limited angular resolution is to be maintained.

The angular pointing tolerances on the aft optics assembly can be calculated based on the tolerance of ±0.1 mm on the lateral positioning of the primary lens with respect to the aft optics. Since the separation of the primary and the aft optics is about 400 m, a lateral offset of the primary lens of 0.1 mm corresponds to a pointing offset of (0.1 mm)/(400 m) = 0.25 µrad. A pointing error or angular jitter greater than this would degrade the blur spot in the focal plane to above the diffraction limit.
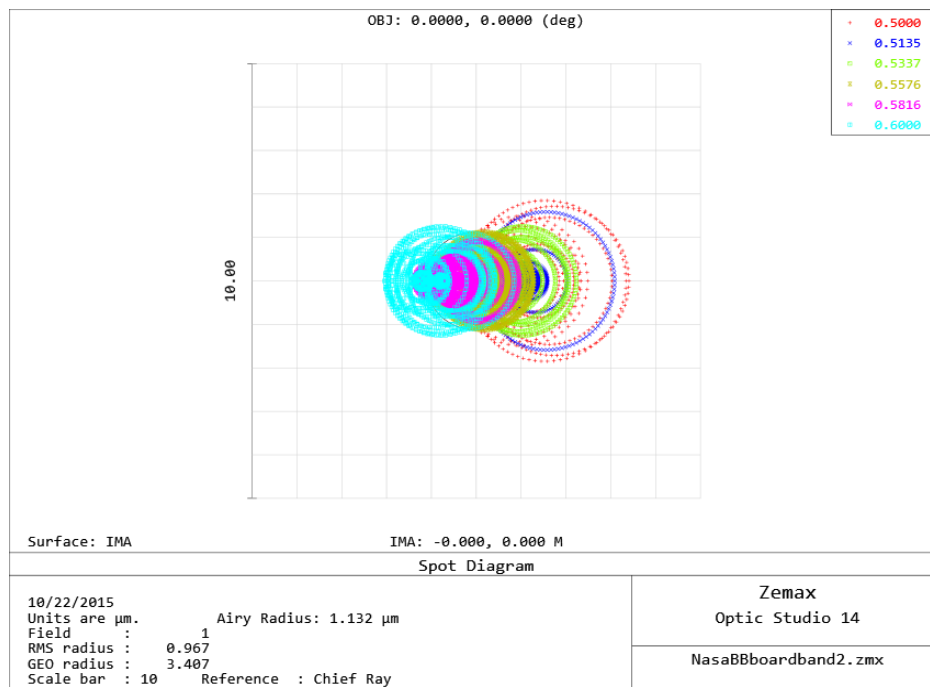

Figure 12. Effect of displacing the primary DW lens by 0.1 mm laterally with respect to the aft optics assembly.

Figure 13 shows the impact on the focal plane blur spot of tilting the primary diffractive lens with respect to the aft optics assembly by 0.005° (87 µrad), indicating the maximum allowable tilt needed to maintain acceptable angular resolution. For this tilt angle, the RMS radius is approximately doubled relative to its value without any tilts or decenters.

Figure 14 addresses the requirement on axial spacing of the primary diffractive lens with respect to the aft optics assembly. The analysis results indicate that axial offsets of up to about 1.5 mm between these two assemblies should be tolerable. For this axial shift, the RMS radius is again approximately doubled relative to the case with no axial shift. This result can be used to derive requirements on station-keeping for concepts in which the two major assemblies fly in formation, without any mechanical connection.
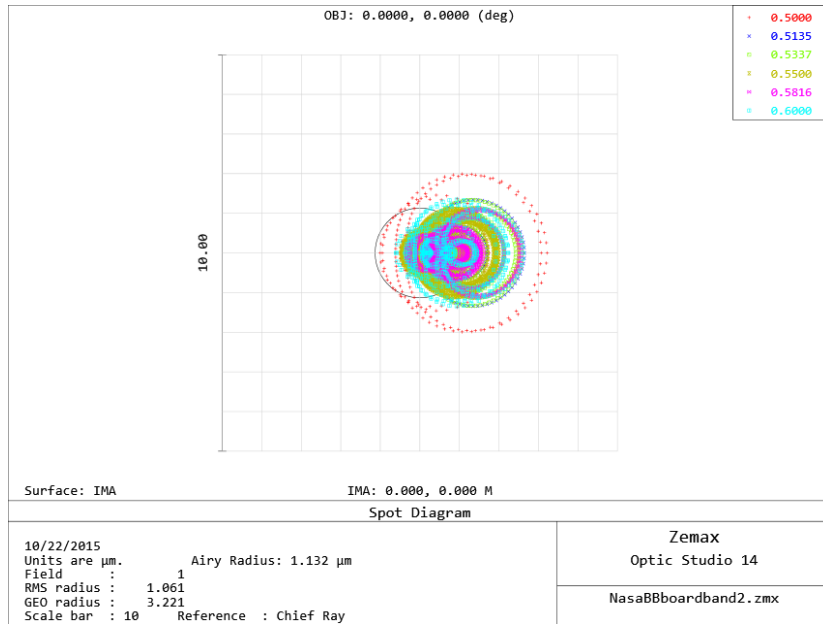
Figure 13. Effect of tilting the primary DW lens by 0.005° (87 µrad) with respect to the aft optics assembly
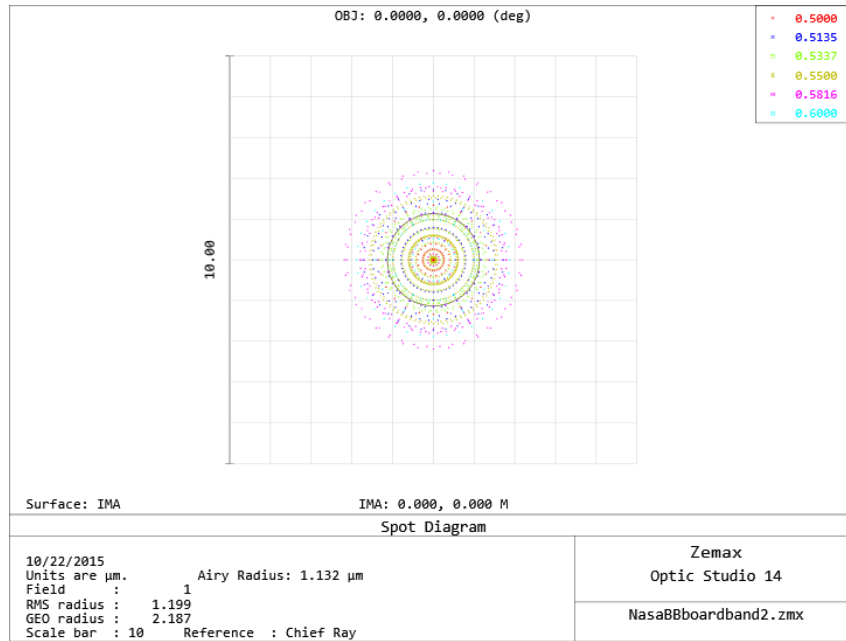

Figure 14. Effect of an axial shift of 1.5 mm between the primary lens and the aft optics assembly.

We have not yet examined the possibility of compensating for relative tilts, decenters, or axial offsets between the primary diffractive lens and the aft optics assembly. It is likely that the tolerances on these parameters can be significantly relaxed if appropriate compensation mechanisms, such as deliberate displacements or tilts of aft optics components, are incorporated into this assembly.

2.3 Feasibility of DW coatings on curved surfaces

Since the concepts we have developed under the Phase I program require diffractive waveplate coatings on curved surfaces, our demonstration of the feasibility of such coatings seems relevant. For the demonstration, we coated eight off-the-shelf plano-concave glass (BK7) refractive lenses by a standard method used with planar surfaces, as illustrated in Figure 15. Essentially, a planar DW lens coating was replicated onto a curved surface. We used one of BEAM Co.'s commercial photoalignment materials, PAAD-72, spin-coated onto the concave curved surface of each of the eight lenses of focal lengths -150, -200, -250, -250, -300, -400, -500 and -700 mm. The diameter of the lenses was 25 mm, of which the central 20 mm diameter was coated to create a DW lens. After photoalignment, an LCP coating was applied and polymerized with UV radiation.
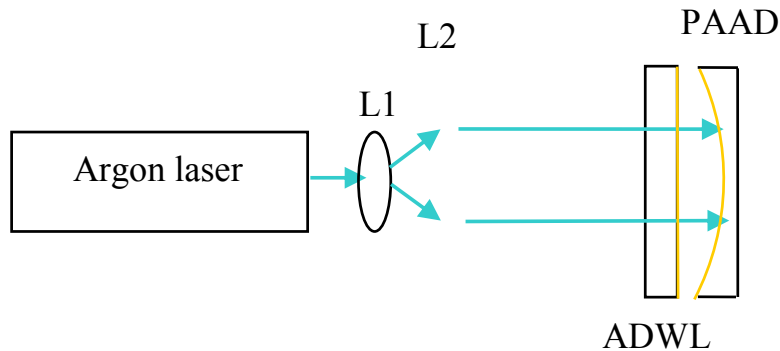

Figure 15. Optical layout for printing a DW lens pattern onto the curved surface of a 25 mm diameter plano-concave lens. L1 and L2 form a collimator for the argon ion laser; ADWL is an LCP achromatic DW lens; PAAD indicates a BEAM Co. photoalignment layer on the concave surface of the refractor.

Figure 16 shows photomicrographs at several locations on the curved surface of the lens with refractive focal length of -500 mm after the DW coating had been applied. Measurements and calculations of focal length vs. wavelength for each polarization at 488 nm wavelength were performed to verify the expected dependence on the focal length of the hybrid refractive-diffractive

lens on the focal length of the underlying refractive lens which served as a substrate for the DW coating. The results of these measurements and calculations are shown in Figure 17.
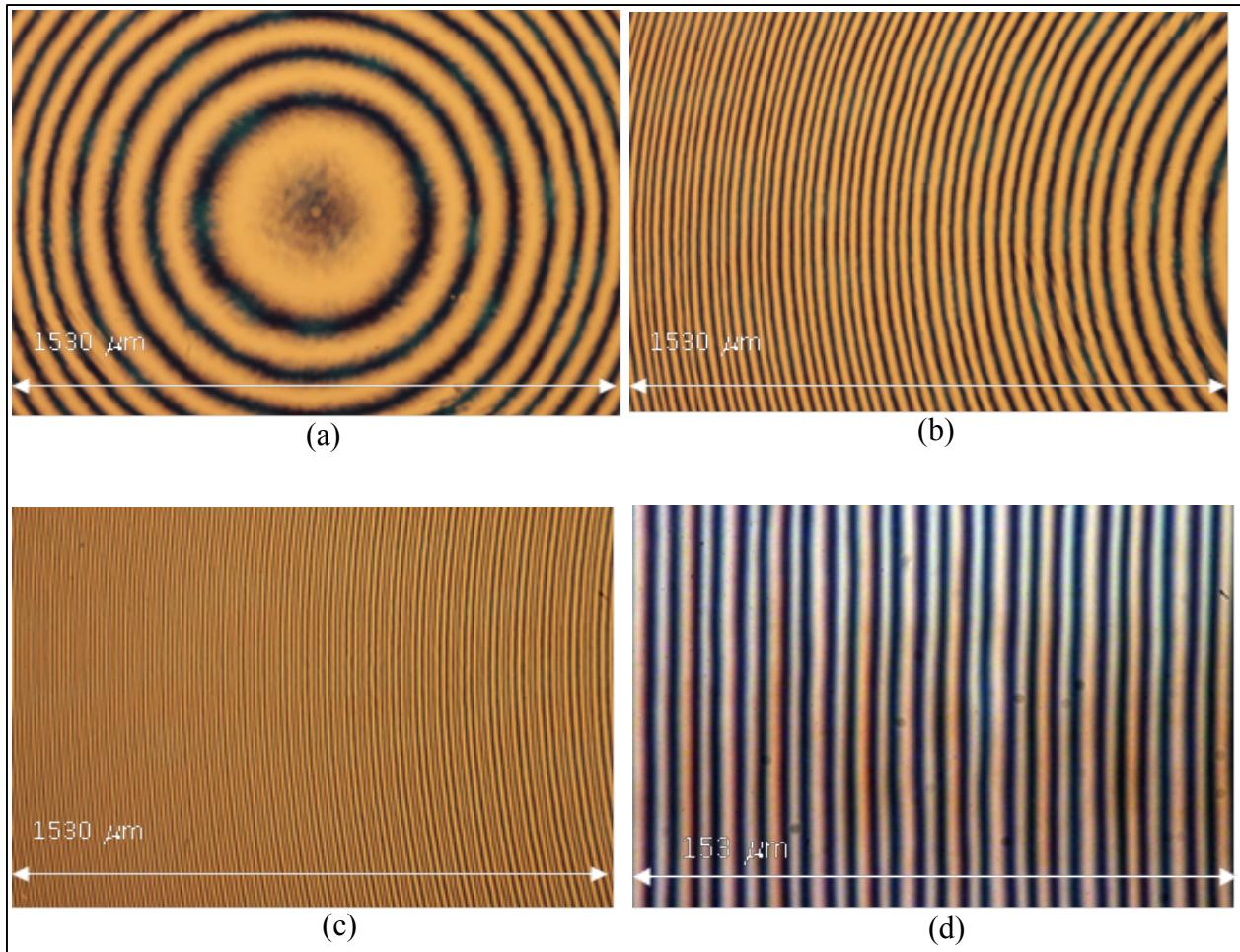

Figure 16. Photomicrographs of DW lens coating on concave surface of a plano-concave lens with a refractive focal length of -500 mm, between polarizers. The focal length of the DW lens coating is 160 mm at a wavelength of 488 nm. (a) Center of DW lens; (b) slightly off center; (c) near the edge of the lens; (d) at the edge of the lens. Period of the DW grating structure at the edge of the lens was 8 μm.

The result of our fabrication of hybrid diffractive-refractive lenses with DW coatings is confirmation that DW coatings on curved surfaces are feasible. Although the demonstration was performed with a refractive lens as the substrate, the conclusion applies as well to DW coatings on mirrors, as is required for the space-based telescope concept described earlier in this report.
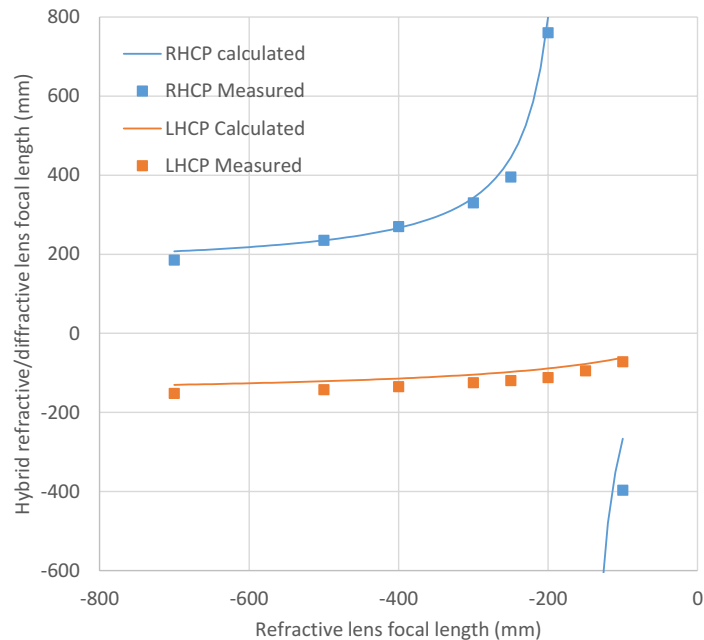
Figure 17. Measured and calculated focal lengths of hybrid refractive-diffractive lenses for the two polarizations of light. Measurements were performed with an argon ion laser beam with a wavelength of 488 nm.

2.4 Alternative optical design with reduced diffraction-limited bandwidth

Our understanding of the possible applications of very large-aperture space-based telescopes is that the wider the operating spectral bandwidth, the better. However, with a diffractive primary mirror, the size of the aft optics (in particular, the diameter of the first corrector mirror) is driven by the required spectral operating bandwidth. We found by means of optical design modeling that in order to achieve a diffraction-limited bandwidth of ±8% of the central wavelength, the diameter of the first corrector mirror has to be 4 m if the primary DW lens has a diameter of 20 m. An optical system with a curved aspheric secondary mirror of this diameter would be a challenge to fabricate with the required optical quality, although such fabrication is not beyond the current state of the art.

We also considered an alternative design with reduced spectral coverage of ±10 nm around 760 nm (oxygen line), and correspondingly reduced aft optics size. The overall layout of this alternative design is illustrated in Figure 18. Although the primary DW lens diameter is 20 m as with the baseline design described above, the diameter of the first corrector has been reduced from 4 m to 1 m. The second corrector mirror is also much smaller than was the case with the baseline design.
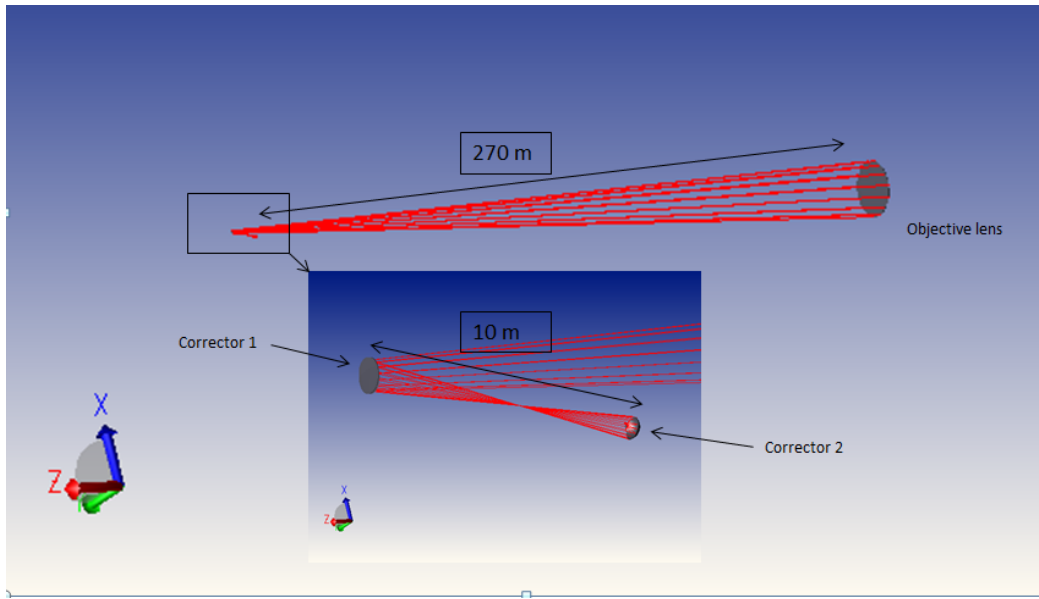
Figure 18. Alternative space telescope design concept with reduced aft optics size. As with the baseline design, the primary DW lens ("Objective lens") is 20 m in diameter, but the diameter of the first corrector mirror ("Corrector 1") has been reduced from 4 m to 1 m.

Figure 19 shows the RMS spot radius as a function of wavelength for the alternative design with 1 meter diameter first corrector mirror. As shown by this figure, the design is diffraction-limited from 749 nm to 774 nm.
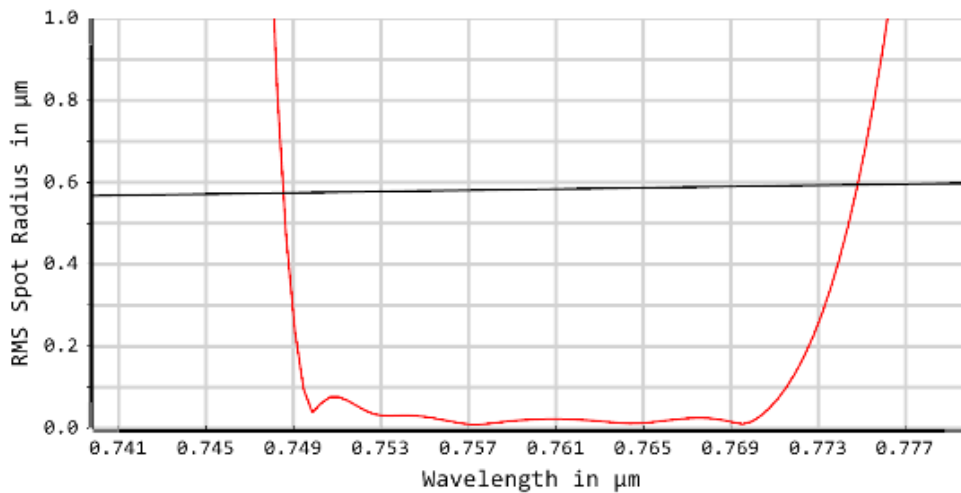

Figure 19. RMS geometric spot radius vs wavelength (red line) relative to Airy radius (black line) for alternative telescope design with reduced aft optics size.

2.5 Multiband concept using multi-layer DW components

Relatively simple scaling considerations can be used to show that our baseline telescope design concept described in the discussion of Figure 5 through Figure 10 could achieve diffraction-limited performance over at least +/-8% of the nominal center wavelength for any selected center wavelength from at least the visible wavelength range through the mid-infrared (i.e. out to at least 6 μm wavelength), limited by the range of transparency of available LCP materials. Issues with available materials for manufacturing diffractive waveplate coatings would result in optical losses that may be unacceptable for wavelength ranges that include wavelengths beyond the mid-infrared, but with some material development it is expected that it will become possible to construct DW-based telescopes with acceptable optical losses operating at longer wavelengths (longer than 6 μm) and shorter wavelengths (shorter than 0.4 μm) than are accessible using current technology. To convert the design from one wavelength band to another wavelength band, it is not necessary to change the shape of the mirrors, it is only necessary to scale the spatial modulation of the diffractive coatings to the new wavelength range, or to design multi-band coatings.

As an illustration of the principle that the diffraction-limited operating band can be shifted without changing the optical element diameters and curvatures, but only changing the DW coating design, Figure 20 shows the predicted focal spot size for two cases. In both cases, the shapes and sizes of all the optics are the same, the only difference between the two cases is the DW coating patterns on the primary DW lens and the two corrector mirrors.

The concept for a multilayer, multiband coating is illustrated schematically in Figure 21. Layer 1 diffracts Band 1 and passes Band 2; Layer 2 passed Band 1 and diffracts Band 2. With such coatings on all the optical components of a design such as the one modeled for Figure 20, both Band 1 and Band 2 would be brought to the same focal plane.

It is known that radical changes in the spectral characteristics of DW coatings can be achieved by means of creating a particular axial dependence in the optical axis orientation, as illustrated earlier in this report in Figure 3. An example of such radical alteration is shown by the measurement results of Figure 22, for a coating designed to have a much broader operating bandwidth than the bandwidth for a simple coating with no axial dependence of the optical axis orientation. The fact that such radical broadening of the operating spectral band is achievable by means of applying a carefully crafted twisted axial structure suggests, but does not prove, that multiband coatings are feasible with an appropriate dependence of optical axis orientation on axial location.

2.6 Polarization-insensitive imaging with DW lenses

We reported in Ref. [9] on optical designs employing DW lenses that bring both polarizations of light to the same focus, despite the fact that the signs of the focal lengths of such lenses are opposite for the two circular polarizations. A conceptual example of this is shown in Figure 23, in which two DW lenses are spaced 5 m apart, and the combination of the two lenses brings light of both polarizations to the same focal point. The obvious advantage of such a

configuration, or a variant of it, is that instead of bringing only 50% of incoming unpolarized light to a given focus, all of the light is brought to the same focus.
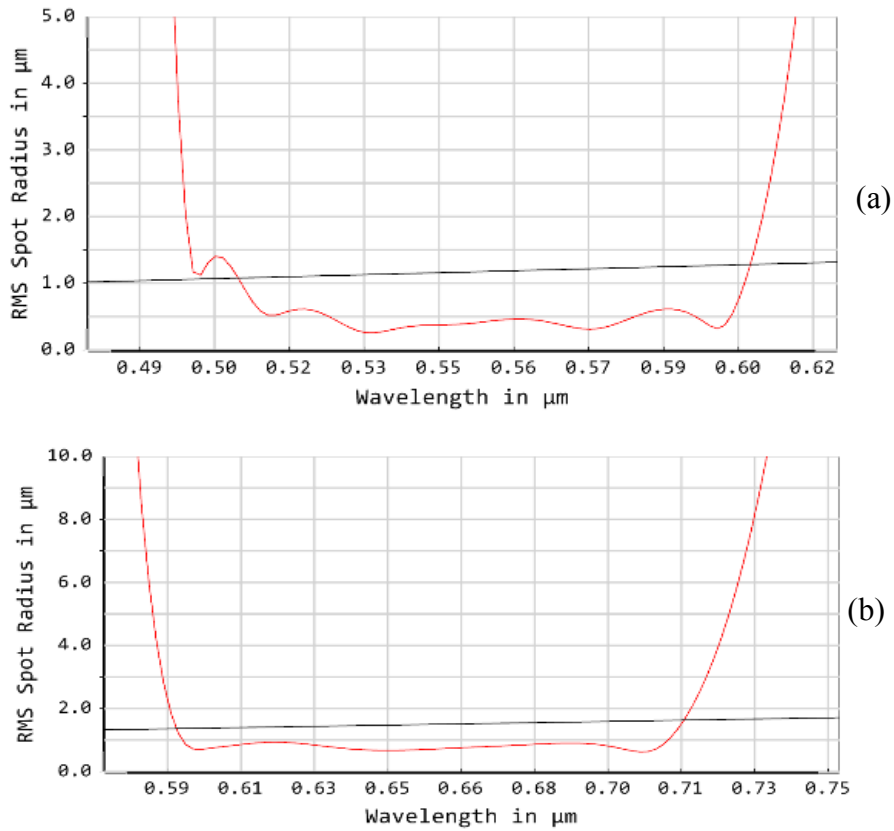

(a)

(b)

Figure 20. Two instances of the baseline telescope, with the same component shapes (including diameters and curvatures), but with coatings optimized for two slightly different bands.(a) Coatings optimized for 0.5 - 0.6 µm; (b) coatings optimized for 0.6 - 0.7 µm.
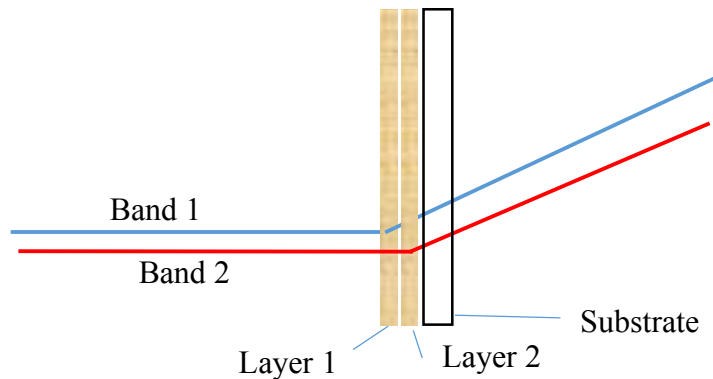

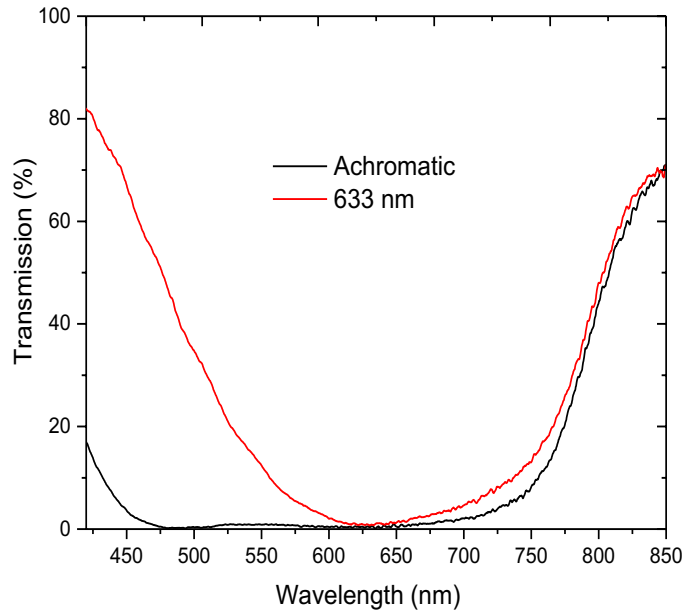Figure 21. Multilayer, multiband coating concept.

Figure 22. Broadband high efficiency diffractive waveplate coatings, from Ref. [11]. Zero-order leakage is shown for an achromatic coating and for a single-layer coating designed for a wavelength of 633 nm.
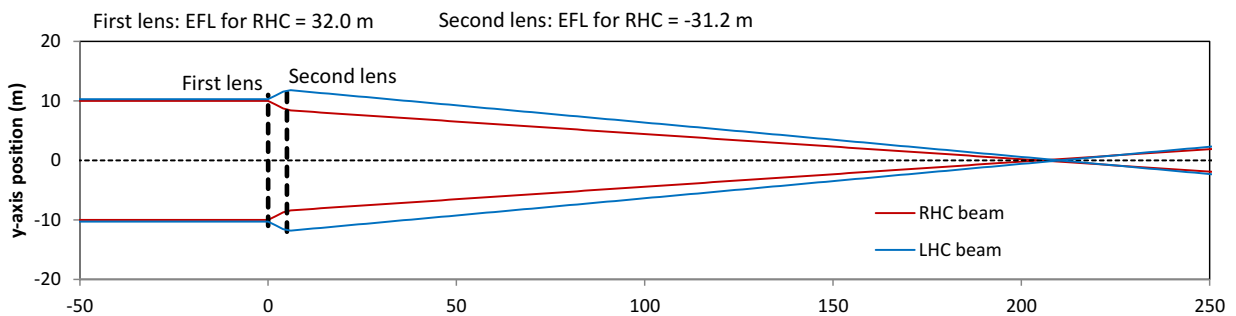

Figure 23. Concept for large-aperture DW lens pair with 100% diffraction efficiency. RHC means right-hand circularly polarized light, EFL means effective focal length. The focal length for LHC (left-hand circularly polarized light) is (-1) times the focal length for RHC for each lens. Polarization shown is the polarization at the input of each component; for clarity, polarization reversals at each lens are not shown in this figure.

We have not yet demonstrated a design concept in which such high-efficiency, polarization-insensitive imaging can be achieved while simultaneously achieving all other requirements including diffraction-limited imaging over a desired spectral band and field angle. However, the doubling of available light over the simpler configuration with a single primary DW lens is sufficiently intriguing to make future study worthwhile.

3. Conclusions and Next Steps

Using standard optimization techniques, we found that achievement of a diffraction-limited spectral bandwidth of ±8% of the center wavelength required a first corrector diameter approximately 20% of the primary lens diameter, and a diffraction-limited spectral bandwidth of ±1.5% of the center wavelength required a first corrector diameter approximately 5% of the primary lens diameter. Other tradeoffs between operating bandwidth and size of the aft optics are also clearly possible.

As reported previously, in the large-aperture diffractive telescope under consideration, the distance from the primary or objective lens to the first corrector mirror is 410 m. As we consider our design options to reduce this separation to a more manageable value, while still retaining a reasonable diffraction-limited spectral bandwidth, we are exploring the option of making the primary lens a part of a structure that is not connected with the structure that contains the other optical components, including the two corrector mirrors and the image sensor. This would require the development of precision station-keeping or "formation flying" of space structures. Our preliminary optical tolerance analysis will be used in Phase II of our program to evaluate the feasibility of such "formation flying" options for a future large-aperture space telescope for use in missions such as exoplanet imaging and analysis.

There are many issues that must be resolved in order to solidify and make credible the concept of using diffractive waveplate optical components in large-aperture space telescopes. We have provided in our Phase I study some preliminary indications that this is an attractive alternative to previously suggested diffractive techniques. The advantages previously discussed regarding practicality of fabrication at an affordable cost, optical efficiency, broadband and multiband capability, continuous mechanical structure with expected manageable forward scattering, and cost savings associated with the ability to coat curved surfaces with DW coatings make this technology extremely attractive for further investigation for NASA applications.

References

[1] S. Pancharatnam, "Achromatic combinations of birefringent plates," Proc. of the Indian Academy of Sciences, Section A **41**(4), 130-144 (1955).

[2] S. Pancharatnam, "Generalized theory of interference, and its applications. Part I. Coherent pencils," Proceedings of the Indian Academy of Sciences, Section A. **44**(5), Indian Academy of Sciences (1956).

[3] M. Berry, "Pancharatnam, virtuoso of the Poincare sphere," Current Science-Bangalore **67**, 220-223 (1994).

[4] N. V. Tabiryan, S. R. Nersisyan, H. Xianyu, and E. Serabyn, "Fabricating vector vortex waveplates for coronagraphy," in *Proceedings of 2012 IEEE Aerospace Conference* (IEEE, 2012), pp. 1-12.

[5] S. R. Nersisyan, N.V. Tabiryan, D. Mawet, and E. Serabyn, "Improving vector vortex waveplates for high-contrast coronagraphy," Optics Express **21**(7), 8205-8213 (2013).

[6] N.V. Tabiryan, H. Xianyu, and E. Serabyn, "Liquid crystal polymer vector vortex waveplates with sub-micrometer singularity," in *Proceedings of 2015 IEEE Aerospace Conference* (IEEE, 2015), pp. 1-10.

[7] N. Murakami et al., "Design and laboratory demonstration of an achromatic vector vortex coronagraph," Optics Express **21**(6), 7400-7410 (2013).

[8] N. Tabirian, S. V. Serak, D. M. Steeves, and B. R. Kimball, "Waveplate lenses and methods for their fabrication," U.S. Provisional Patent Application No. 61/801,251, March 15, 2013; N. Tabirian, S. V. Serak, D. M. Steeves, and B. R. Kimball, "Waveplate lenses and methods for their fabrication," U.S. Patent Application No. 14/214,375, March 14, 2014 (to be published).

[9] N. V. Tabiryan, S. V. Serak, D. E. Roberts, D. M. Steeves, and B. R. Kimball, "Thin waveplate lenses of switchable focal length - new generation in optics," Optics Express **23**(20), 25783-25794 (2015).

[10] N. V. Tabiryan, S. V. Serak, , D. E. Roberts, D. M. Steeves, and B. R. Kimball, "Thin waveplate lenses: new generation in optics," Proc. SPIE **9565**, 956512 (2015).

[11] N. V. Tabiryan, S. V. Serak, S. R. Nersisyan, D. E. Roberts, B. Ya. Zeldovich, D. M. Steeves, and B. R. Kimball, "Broadband waveplate lenses," Optics Express (accepted for publication).

[12] N. V. Tabiryan, "Breakthrough in Optical Sensor Protection and Laser Beam Control Systems," 2014 Meeting of the Military Sensing Symposium Specialty Group On Active E-O Systems, Washington D.C., August 25-28, 2014.

[13] N. V. Tabiryan, "The 4th Generation of Optics," Cooperation on Science and Technology (COST) meeting, Prague, Czech Republic, September 18-19, 2014.

[14] N. V. Tabiryan, S. V. Serak, D. E. Roberts, E. Serabyn, D. M. Steeves, and B. R. Kimball, "Ultralight and inexpensive telescope technology for deep space optical communication," 12th Mediterranean Workshop and Topical Meeting on Novel Optical Materials and Applications (NOMA 2015), Cetraro, Italy, June 7-13, 2015.

[15] N. V. Tabiryan, S. V. Serak, D. E. Roberts, E. Serabyn, D. M. Steeves, and B. R. Kimball, "Novel opportunities for controlling light with liquid crystals," Gordon Research Conference, Liquid Crystallinity in Soft Matter at and Beyond Equilibrium, Biddeford, Maine, June 21-26, 2015.

[16] N. V. Tabiryan, "The next horizon for diffractive waveplate technology," Keynote presentation at SPIE's Optics & Photonics Symposium, San Diego, CA, August 2015.

[17] N. V. Tabiryan, "The Fourth Generation of Optics," Opening Keynote Address at Eurodisplay 2015.

[18] N. V. Tabiryan, "Superlens in the skies: Liquid crystal polymer telescope technology development," (Invited Paper), presentation at SPIE Photonics West, San Diego, CA, February 16, 2016.

[19] K. Gao, H. H. Cheng, A. K. Bhowmik, and P. J. Bos, "Thin-film Pancharatnam lens with low f-number and high quality," Optics Express **23**(20), 26086-26094 (2015).

[20] A. M. W. Tam, F. Fan, H. S. Chen, D. Tao, V.G. Chigrinov, H. S. Kwok, and Y. S. Lin, "Continuous Nanoscale Patterned Photoalignment for Thin Film Pancharatnam-Berry Phase Diffractive Lens," SID Symposium Digest of Technical Papers **46**(S1), p. 8 (2015).

[21] J. Kim, Y. Li, M. N. Miskiewicz, C. Oh, M. W. Kudenov, and M. J. Escuti, "Fabrication of ideal geometric-phase holograms with arbitrary wavefronts," Optica **2**(11), 958-964 (2015).

[22] R. A. Hyde, "Large Aperture Fresnel Telescopes," Lawrence Livermore National Laboratory Report UCRL-ID-131320 (1998).

[23] R. A. Hyde, "Eyeglass. 1. Very large aperture diffractive telescopes," Applied Optics **38**(19), 4198-4212 (1999).

[24] U.S. Department of Defense, Contracts Announcement No: 759-11, September 2, 2011, http://defensenews-updates.blogspot.com/2011/09/dtn-news-us-department-of-defense_02.html

[25] J. L. Domber, P. D. Atcheson, and J. Kommers, "MOIRE: ground test bed results for a large membrane telescope," in *Proceedings of 2014 Spacecraft Structures Conference* (AIAA, 2015), pp. 1-17.

[26] J. A. Britten et al., "Large-aperture fast multilevel Fresnel zone lenses in glass and ultrathin polymer films for visible and near-infrared imaging applications," Applied Optics **53**(11), 2312-2316 (2014).

[27] L. Koechlin et al., "First high dynamic range and high resolution images of the sky obtained with a diffractive Fresnel array telescope," Experimental Astronomy **33**(1), 129-140 (2012).

[28] G. P. Andersen and O. Asmolova, "FalconSAT-7: a membrane space telescope," Proc. SPIE **9143,**, 91431X (2014).

[29] A. Heller, "A giant leap for space telescopes," Science and Technology Review, March 2003, pp. 12-18. Lawrence Livermore National Laboratory.